ALMA 2015 : STUDY AND MODELING OF THE IMPULSE RESPONSE VERTICAL DE-COHERENCE IN A FLUCTUATING SHALLOW CHANNEL

Iannis Bennaceur[a], Xavier Cristol[a], Bruno Chalindar[a]
Gaultier Real[b], Dominique Fattaccioli[b]

[a]THALES Defense Mission Systems France
[b]DGA Naval Systems

525 route des Dolines, 06560 Valbonne FRANCE.
iannis.bennaceur@fr.thalesgroup.com

Abstract: *Before reception by a sonar array, acoustic signals of interest are strongly altered during propagation through the unstationary inhomogenous random sea. Some configurations, like shallow waters, are particularly impacted by strong stochastic fluctuations of the sea features and much work is still needed to understand, model and mitigate the effects of random acoustic propagation on the sonar performance.*
Acoustic propagation in shallow water is investigated using signals collected by the "ALMA" (Acoustic Laboratory for Marine Applications) system deployed in 2015 by DGA Naval Systems, in the Mediterranean Sea. The 2015 instrument configuration combined an acoustic source transmitting different types of wide- and narrow-band pulses over the 2 to 11 kHz band, and a 10 meter high receiving vertical array of 64 hydrophones. The main topic of this article is the experimental study of the vertical loss of coherence of the received signals, which would have an impact on sonar performance. The first step of the work was to evaluate the impulse response and a vertical coherence characteristic length using the pulses propagated through the stochastic fluctuating channel in a relatively calm-sea configuration. Then, the observed impulse responses and the coherence scales are simulated with the in-house stochastic numeric tool NARCISSUS and compared to the experimental measurements.

Keywords: *Underwater acoustic modelling, vertical coherence, shallow-water acoustic propagation*

1. INTRODUCTION

There is some confusion around the use of the word "*coherence*" in physics of waves and radiation. This term appears in at least three interconnected semantic fields. Firstly, the "historical" use, arising from the early XIX° century optics, applies to the capability of waves, radiating sources or experimental devices to produce observable interference effects (fringes, beatings). Secondly, in a "statistical" sense, "*coherence*" or "*coherence function*" may stand as synonyms to the "cross-correlation" of a wave field in phase and amplitude, *i.e.* the expectation of the product of the complex wave amplitudes taken at two locations, two times, or two frequencies, and considered as a function of the lag in location, time or frequency. In a third "cognitive" definition, "*coherence*" refers to the possibility for an intelligent agent to predict the state of a physical system at some arbitrary time or location, from the preliminary knowledge of its state at a first time or location; this prediction must rely on a practically tractable, deterministic model, involving not too high a number of degrees of liberty. In the LF and HF sonar or radar fields, "coherent processing" generally assumes a predicting model, according to which delayed versions of the same waveform are observed at different locations along wave-fronts with simple geometries (plane, spherical), at least over the span of an array.

According to these three definitions, the *lack* or *loss of coherence*, or *de-coherence*, or *partial coherence*, may refer to three different, but mutually related phenomena: 1) the smoothing, instability or disappearance of interferences; 2) a cross-correlation function featuring significant non-zero values only over a narrow domain; 3) an inadequate prediction model of the variations of the considered physical system, 'inadequate' meaning that a correct model should be either stochastic, or deterministic with a very high, virtually infinite number of degrees of liberty. We will explore the last two conceptions of de-coherence for sonar applications and the capability to model them numerically, using data from the 2015 ALMA experiment,

"ALMA" (Acoustic Laboratory for Marine Applications) is a deployable and autonomous acoustic and environmental system, with passive and active sub-systems; it was designed by the French Defence Procurement Agency to address the main topics of underwater acoustics by gathering real environmental and acoustical data for developing and validating advanced signal processing algorithms and acoustic models [1]. From 2014 to 2018, five large scale campaigns were conducted in the Mediterranean Sea and the Atlantic Ocean, evoked in various publications ([2], [3], [4]). In this paper, we use some of the data collected during the 2015 ALMA campaign to investigate the vertical de-coherence of the acoustic field after propagation through a randomly fluctuating shallow channel.

2. THE "ALMA 2015" EXPERIMENTAL CONFIGURATION

The 2015 ALMA campaign was conducted from the 5th to the 10th of November 2015 in a shallow Mediterranean environment, over a 100m-deep, gently sloping, sandy-gravely continental shelf, near the French harbor of Toulon. The acoustic system consisted in a moored active source and a moored vertical 10-meter high array of 64 hydrophones, separated by 9.11 km and immersed at approximately 56 m (see *Fig.1(a)*). The source transmitted, among others waveforms, 1-second long continuous waves (CW) at the frequencies 2, 5, 7 and 11 kHz and 2-seconds long linear frequency modulated (LFM) pulses over the 4-6 kHz band. During 20 hours, 415 pings were emitted, including 2 CW for each frequency and 2 LFM transmissions, every 3 minutes. The sound-speed profile measured close to the source, on the 6th of November, is almost iso-thermal over the first 50 m, and suddenly decreases quite sharply and irregularly down to the seabed (see *Fig.1(b)*).

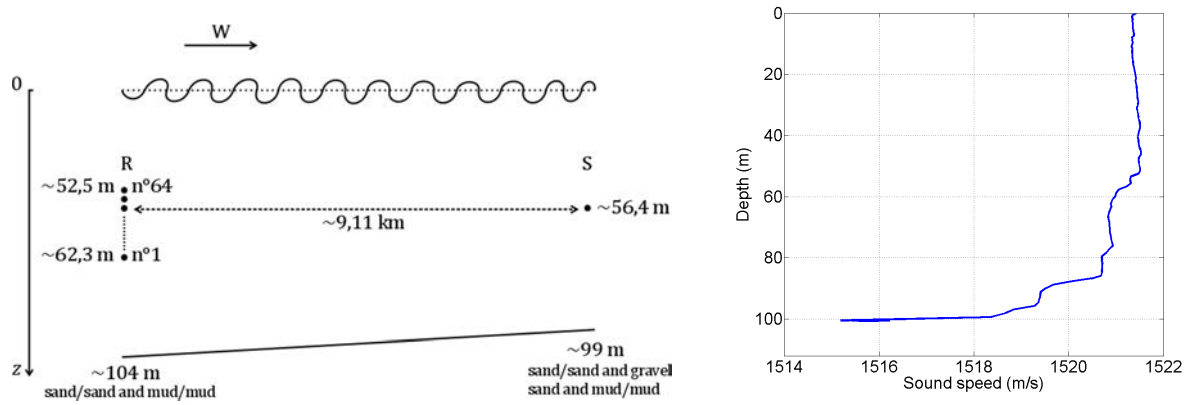

(a) *(b)*

Fig.1: (a) Experimental ALMA 2015 configuration. (b) Sound-speed profile near the source.

We have firstly observed a particularly favorable period of 5 hours (~100 pings), during the night, over which the signal-to-noise ratio was high: a smooth well-aroused swell, corresponding to a sea-state 1.5-2, coinciding with a low wind velocity, resulted in a very low noise level (less than equivalent to sea-state 1). After sunrise, the rest of the experiment was unfortunately corrupted by intense bursts in sea-noise, due to the diurnal near shipping and to higher wind velocities.

3. PRELIMINARY ANALYSIS OF THE CHANNEL IMPULSE RESPONSE

In this section, we present a first investigation of the structure of the Impulse Response (IR) of the channel over all receivers of the array, estimated from 4-to-6kHz LFM pulses as the output from the matched filtering; this estimated IR is then compared to the IR simulated with an in-house stochastic numerical tool named NARCISSUS.

The three grey mappings of *Fig.2* display the level of the estimated IR issued from the pings 40, 137 and 143, as a function of the hydrophone depth (vertical axis) and of the time delay (horizontal axis). The ping 40 was emitted when the sea was calm, the 137 when it was slight and the 143 when it was moderate. The reference time delay 0 ms is taken at the time for which the vertically averaged impulse response is maximum. The IR associated with the ping 40 presents a first highly energetic arrival (A_1), followed by a 10-second highly fluctuating cluster (B), and some more later arrivals (A_2 at 20 ms and A_3 at 27 ms), less energetic than A_1 and slightly tilted. When the sea-surface roughness grows (pings 137 and 143), the most energetic arrival may not be the first one. Moreover, the levels of late arrivals decrease for the benefit of scattered 'reverberated' energy, filling the time intervals between late arrivals (especially for the ping 143).

For our comparison with the modelled IR, we have computed an averaged IR response over 30 pings emitted when the sea was calm (sea-state of 1.5) and the noise level particularly low. Due to the verticality of the late arrivals, averaging was performed first over the receiver depth, and then over the pings. The resulting averaged IR is displayed by the dark line of *Fig.4*, along with a measure of the dispersion over the pings (± standard deviation).

We have otherwise simulated the impulse response of the channel using NARCISSUS which computes, with a Monte-Carlo technic, the sea-surface and bottom scattering of an acoustic field emitted at more than about 500 Hz. The acoustic kernel, that described acoustic scattering from surface roughness, is evaluated using the "integral small-slope approximation" (or "Meecham-Lysanov approach", see [5], pp. 191-194); the surface height fluctuations are computed with the JONSWAP model ([6],[7]) and we use the Beckmann

approximation to model the scattered field spectrum. The seabed is inhomogeneously composed of sand, mud and gravel, which we described by a median porosity of 55% and a roughness of 0.15 m. When the surface roughness (standard deviation of height) is set to 0.094 m, well-fitting to the sea-state 1.5, a good agreement between the averaged measured IR and the simulated one is obtained, as demonstrated by Fig.3.

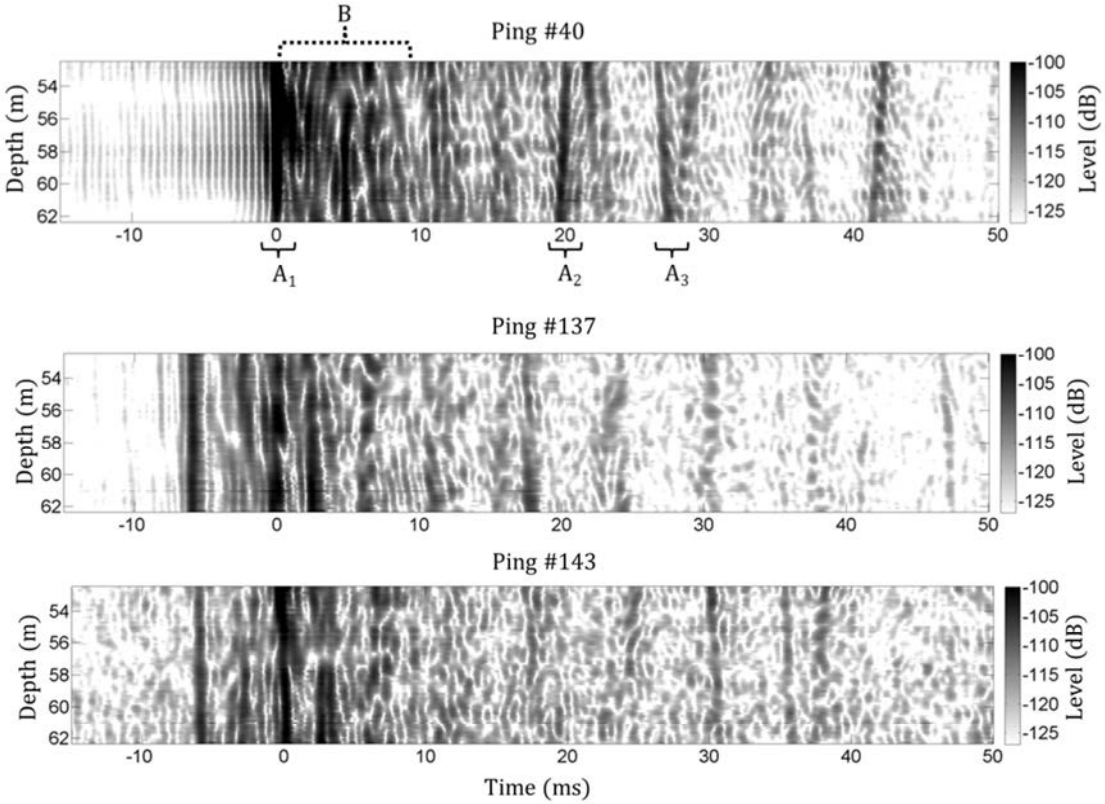

Fig.2: Impulse response of the channel under LFM pulses at the output of the matched filter emitted at the ping 40, 137and 143.

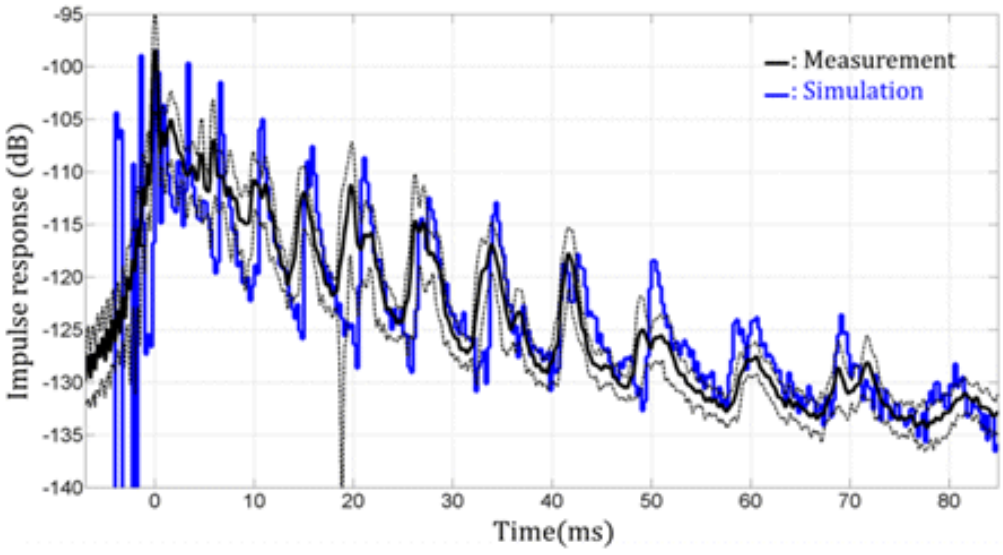

Fig.3: Averaged measured IR: (---) and the simulated with NARCISSUS: (---).

4. OBSERVATION AND PREDICTION OF VERTICAL COHERENCE

4.1. Coherence for CW pulses

In the "statistical" meaning of coherence, we investigate the cross-correlation of the acoustic pressure between all pairs of receivers for the CW pulses. A processing for measuring a typical vertical coherence scale is the following one: firstly, we get the maximum value of the matched filter output for each hydrophone and each pulse; secondly, we compute the cross-correlation matrix averaged over the 200 harmonic pulses emitted during the calm sea period (we get *Fig.5(a)* for $f = 2$ kHz); finally, we average the cross-correlation matrix over the receivers after having re-centred the matrix around its diagonal (see *Fig.5(b)*). We then define the –3dB vertical coherence length $L_{-3\mathrm{dB}}$ as the length corresponding to a decrease of 3dB from the maximum of the averaged cross-correlation coefficient.

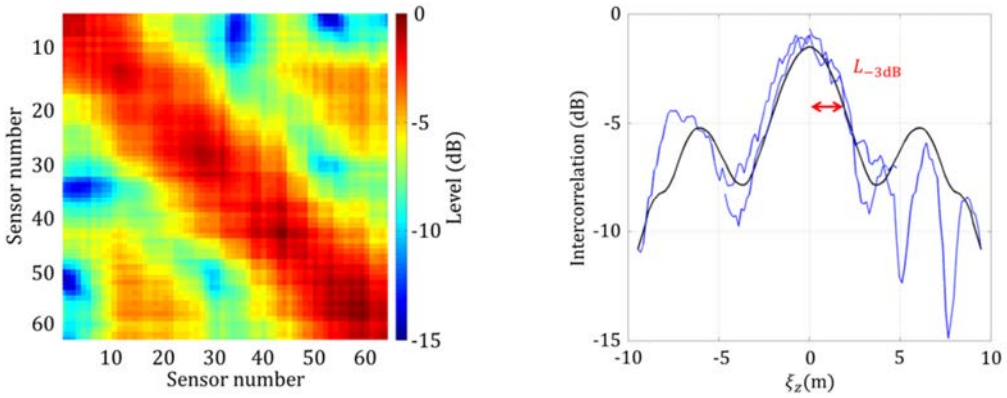

(a) *(b)*

Fig.4: (a) Averaged cross-correlation matrix over the 200 pulses of the CW at 2 kHz. (b) Averaged cross-correlation matrix at sensors 1, 34 and 64: (---) and cross-correlation coefficient issued from an average over the hydrophones: (---).

The values of $L_{-3\mathrm{dB}}$ for $f = 2$ kHz, 5 kHz, 7 kHz, and 11 kHz are 2 m, 1.16 m, 0.88 m, and 0.6 m respectively. Plotted against the normalized length ξ_z/λ (where λ stands for the emitted wavelength), the four cross-correlation functions roughly coincide (*Fig.5*); the vertical coherence length is then close to proportional to λ as could be expected. We find $L_{-3\mathrm{dB}} \approx 4\lambda$.

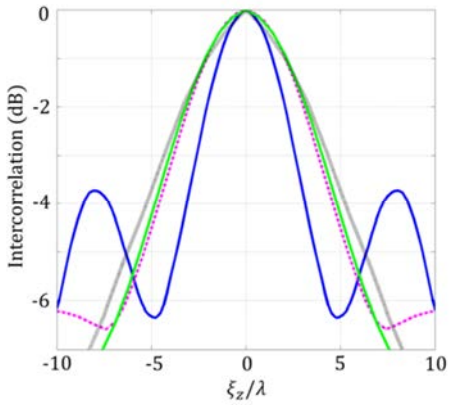

Fig.5: Averaged cross-correlation over the hydrophones against the normalized length ξ_z/λ computed for $f = 2$: (—), 5: (-- --), 7: (—) and 11 kHz: (· · ·).

4.2. Coherence for the individualized arrivals for the LFM pulses

The vertical coherence of the channel's IR according to the "cognitive" meaning may be investigated by using the matched filter outputs computed upon the LFM pulses. The acoustics arrivals occur in two different groups, as observed in section 3: well-separated individualized arrivals, and an early fluctuating cluster. In this study, we try to evaluate the vertical coherence length of both groups and compare it to the coherence length predicted by the numerical model NARCISSUS. We start with the late, strongly individualized arrivals.

After reflection at the random rough sea-surface, wave-fronts have no more simple shapes, but feature complex random undulations around those simple shapes; the description of those stochastic oscillations would require a virtually infinite number of degrees of freedom, and defies deterministic description; the loss of coherence impacting a processing like beamforming is due to the ignorance of those unknown descriptive parameters. The coherence of an arrival has then to be evaluated like in section 3, but around a simple trend most fitted with the descriptive parameters that are taken in consideration: for instance, the two independent parameters that determine a straight line, valid for describing a "mean" wave-front over a short array length.

The processing for quantifying the vertical coherence length of the late arrivals is then as follows. We interpolate the impulse response over a set of variable incidence straight lines around the forthright arrival (yellow lines on *Fig.6*) and we get the line for which the IR level, averaged upon the immersion, is the highest (red line *Fig.6*). This gives us the matched filter outputs for each hydrophone, each pulse and each arrival. To evaluate $L_{-3\mathrm{dB}}$, we then follow the same method as the one described previously for CW pulses.

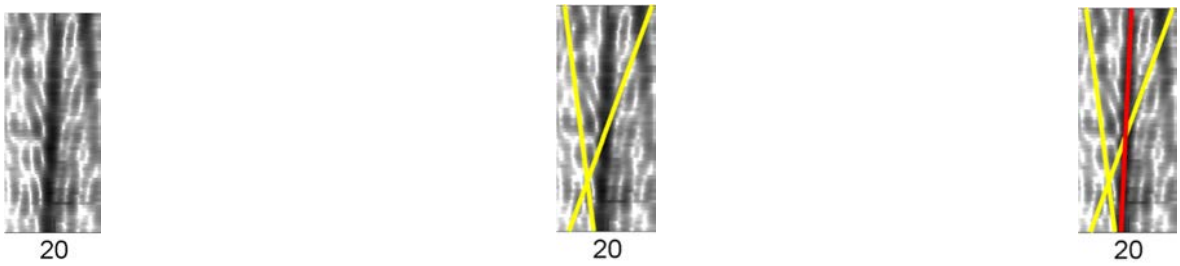

Fig.6: Sketch of the method to evaluate the vertical coherence length of forthright arrivals.

The three plots of *Fig.7* display the cross-correlation functions of arrivals A_1, A_2 and A_3. For the most energetic arrival A_1, the cross-correlation decrease does not exceed 3dB along the 10-meter high array. For the later arrivals A_2 and A_3, a decrease of 3dB occurs at shorter lags, about 3 m and 4.05 m respectively.

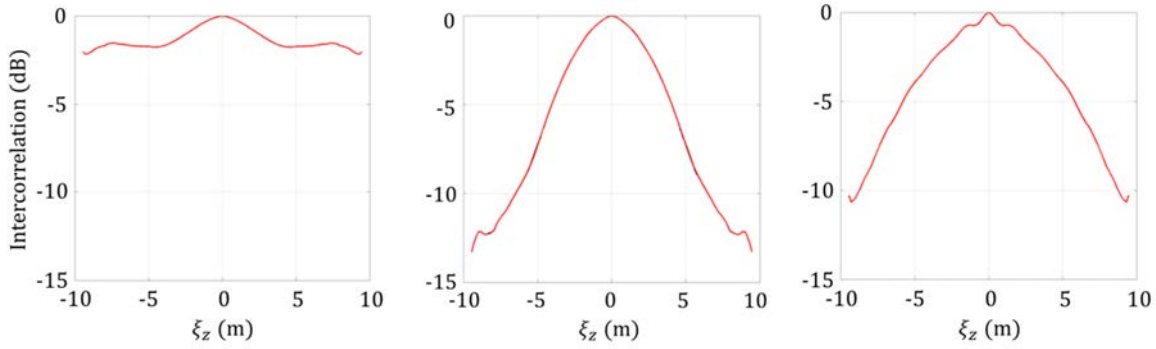

(a) *(b)* *(c)*

Fig.7: Cross-correlation coefficient matrix of the arrivals (a): A_1, (b): A_2 and (c): A_3.

With NARCISSUS, we are able to compute the vertical coherence scale L_N, defined as the half-width of the second-order moment of the probability density function of the impulse response, which is not exactly equal to $0.5\,L_{-3\mathrm{dB}}$. However, it is still interesting to see if NARCISSUS is able to predict the rise of the vertical coherence of the pressure field when a forthright arrival reaches the array. On *Fig.8*, we observe a strong increase of L_N around the delay 27 ms that reaches 2 m, corresponding to the arrival A_3. Such observation would indicate that $L_{-3\mathrm{dB}} \approx 2\,L_N$. We also guess a slight increase between 17 and 20 ms that could correspond to A_2. Here we see that NARCISSUS is an appropriate tool to predict the variation of vertical coherence scale.

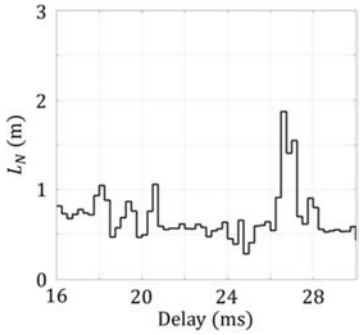

Fig.8: Vertical coherence length issued from NARCISSUS.

4.3. Coherence for the early fluctuating cluster for the LFM pulses

Measuring the vertical coherence length of the fluctuating cluster B is not an easy task, since there are no stable, individualized arrivals that can be easily isolated. Our method here is to sub-divide the impulse response into 0.25 ms wide time-cells (white dot on *Fig.9*) and to apply the same procedure as the one used for the individualized arrivals for each time-cell. We limit to less than 10° the module of the incident angle α of the mean straight line used for the interpolation (*Fig.9*). This processing results in $L_{-3\mathrm{dB}}$ and α according to the delay associated with each cell.

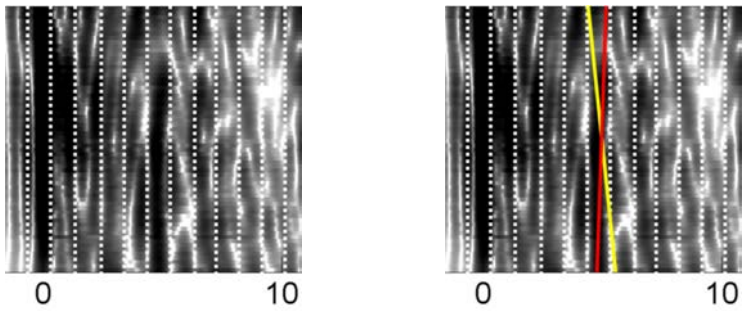

Fig.9: Sketch of the method to evaluate the vertical coherence length of the fluctuating cluster.

We plot these two quantities on *Fig.10*, along with the coherence scale L_N and the incidence angle issued from NARCISSUS. We see that both our evaluation method and NARCISSUS predict a very strong vertical coherence for the time 0 ms corresponding to the most energetic arrival A_1. Moreover, both approaches reveal an increase of the vertical coherence length around 5.5 ms, which probably corresponds to the arrival visible on *Fig.9*. Furthermore, our evaluation method does not seem relevant to correctly evaluate the incidence angle.

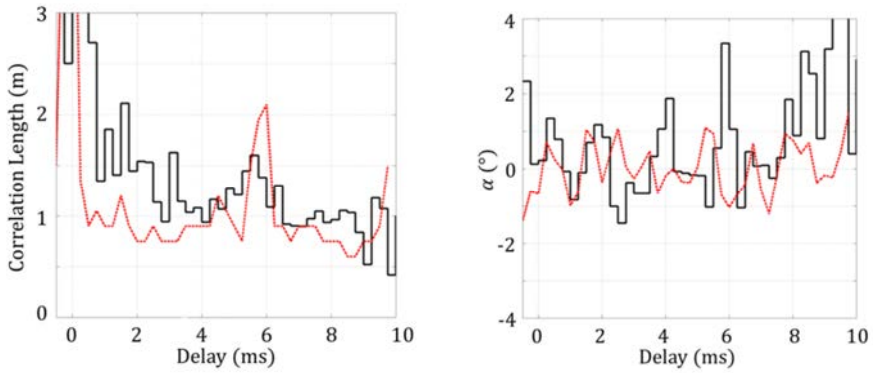

(a) *(b)*

Fig.10: (a) Vertical coherence length and (b) incidence angle of the fluctuating cluster against time measured: (- -) and issued from NARCISSUS: (---).

5. CONCLUSION

In this paper, we studied the vertical de-coherence of wide and narrow-band pulses over the 2 to 11 kHz band that propagated through a fluctuating shallow channel over 9 km. Environmental data collected on the experiment site allowed a relevant estimation of the channel characteristics, in particular the roughness of the sea-surface and the roughness and porosity of the seabed. Then, we observed the measured impulse response depending on the sea-state and we noticed two distinct features; quasi-vertical individualized arrivals and a strongly fluctuating cluster. In the meantime, we have successfully simulated the impulse response using the stochastic numerical tool NARCISSUS using the channel characteristics. Finally, we have estimated the vertical coherence lengths of the CW pulses and of the LFM pulses features. These were compared quite favourably to the coherence scales issued from NARCISSUS.

6. REFERENCES

[1] **Fattaccioli D., Real G.**, The DGA "ALMA" project: an overview of the recent improvements of the system capabilities and of the at-sea campaign ALMA-2016, In *UACE Proceedings*, 2017.

[2] **Cristol X., Real G., Fattaccioli D., Chalindar B.**, ALMA 2014: Observations of Multiple Sound Scattering from Random Inhomogeneities Transported by a mean flow, In *UACE Proceedings*, 2017.

[3] **Bennaceur I., Cristol X., Docquois R., De Pampelone F-R.**, Target Localization in Depth and Range from Passive Sonar, In *Ocean*, 2018.

[4] **Real G., Fattaccioli D., Bennaceur I., Cristol X.**, ALMA, a tool to study sound propagation in fluctuating oceans: latest evolutions and analyses, In preparation for *Ocean*, 2019.

[5] **Voronovitch A. G.**, *Wave scattering from Rough Surfaces*, Berlin: Springer-Verlag, 1994.

[6] **Hasselmann K., Ross D. B., Müller P., Sell W.**, A parametric Wave Prediction Model, *Journal of Physical Oceanography*, volume (6), pp. 200-228, 1976.

[7] **Carter D. T. J.**, Predictions of Wave Height and Period for a Constant Wind Velocity using JONSWAP Results, *Oceanic Eng.*, volume (9), pp. 17-33, 1982.